*Physical Science International Journal*

*17(2): 1-11, 2018; Article no.PSIJ.35306*
*ISSN: 2348-0130*

# Mechanism of Flow in Patchy Gravel and Vegetated Beds

**O. P. Folorunso[1*]**

*[1]School of Civil Engineering, University of Birmingham, Edgbaston, B15 2TT Birmingham, United Kingdom.*

***Author's contribution***

*The sole author designed, analyzed and interpreted and prepared the manuscript.*

***Article Information***

DOI: 10.9734/PSIJ/2018/35306
Editor(s):
(1) Thomas F. George, Chancellor / Professor Department of Chemistry and Physics, University of Missouri-St. Louis, Boulevard St. Louis, USA.
(2) Yang-Hui He, Professor of Mathematics, City University London, UK and Chang-Jiang Chair Professor in Physics and Qian-Ren Scholar, Nan Kai University, China and Merton College, University of Oxford, UK.
Reviewers:
(1) Jordi Colomer, University of Girona, Spain.
(2) Lung-Chien Chen, National Taipei University of Technology, Taiwan.
(3) Eliton da Silva Vasconcelos, Federal University of São Carlos, Brazil.
Complete Peer review History: http://www.sciencedomain.org/review-history/23270

***Original Research Article***

***Received 5th July 2017***
***Accepted 13th August 2017***
***Published 21st February 2018***

## ABSTRACT

Velocity and turbulence measurements were performed in an open channel with patchy gravel and vegetated beds in order to further understand the transport processes and flow regimes that exist in open channels. The results of laboratory experiments that describe the mechanisms and transport features of heterogeneous flexible and rigid strip vegetation flow interaction with gravel roughness are presented. The paper examines the shear layers and momentum transport that arise as a result of a particular type of patchy roughness distribution. It is shown that relative to a gravel bed, the vegetated section of the channel generally resembles a free shear layer. The resistance within the vegetation porous layer reduces the velocity and creates a sharp transition across the interface at the top of vegetation; of primary importance is the shear layer at the top of the vegetation which influences and dominates the overall momentum transport. At the boundary between the gravel and vegetated section, the lateral momentum transport $(-\overline{u'v'}/\tau_b)$ is observed to be a maximum. The Sweep motions are more significant near bed while Ejections dominates the flow at the upper region of the flow.

*Keywords: Vegetation; shear layer; roughness; resistance; turbulence; gravel.*

**Corresponding author: E-mail: ftobex@ymail.com;*

## 1. INTRODUCTION

The presence of vegetation in open channels and in environmental aquatic flows has been recognized to be important for the balance of river ecosystems, e.g., through the provision of river restoration and stabilization of channels [1,2] To predict accurately the conveyance capacity in open channels, it is important to understand the hydrodynamic interaction of the flow with the boundary.

Changes in the shape or resistance characteristics of a channel boundary can induce a change in the flow characteristics [3,4,5]. The velocity profile can become distorted with shear being created at the interface between roughness elements, leading to additional sources of turbulence [6] investigated the effect that changes in bed roughness can have on the mean and turbulence characteristics of the velocity field. This work highlighted the importance that the rough-smooth boundary (i.e., the location where the bed roughness changed) has on the overall momentum transfer and vorticity generation. The research outlined below, extends the work of [4] by considering the effect that idealised vegetation can exert on the main flow characteristics in a heterogeneous channel. In what follows, a detailed investigated of the flow characteristics will be presented for the particular case where the channel bed is composed of heterogeneous roughness formed using gravel and idealised vegetation. However, before these results are presented it is worth briefly considering the fundamental basics of canopy flow since this will provide a framework in which the results can be interpreted.

The distribution of vegetation elements within a canopy can significantly affect the behaviour of the flow [7]. In a sparse canopy (see Fig. 1 for definition), the velocity follows a turbulent boundary layer profile with the bed contributing to the vegetation roughness [7]. In a dense canopy (Fig. 1c), the vegetation drag is larger than the bed shear stress; the flow at the top of vegetation produces a free shear layer through an inflection point near the top of the canopy which leads to flow instability and the additional creation of vortices [8,7]. The vegetation stem density defines the transition from sparse to dense limits with scale $ah$, where $a$ is the stem frontal area, and $h$ is the vegetation height.

### 1.1 Aims and Objectives

Despite the excellent work undertaken by [7] and [4,6], the interaction of vegetation with other forms of roughness is still poorly understood. Hence, the overall aim of the current research, is to evaluate how the dynamics of the flow field change when heterogeneous roughness involving vegetation is present. Related to this the research has the following objectives:

- To investigate the influence that rigid vegetation (akin to 'shrubs') and flexible vegetation (akin to 'grass') have on turbulence generation within an open channel.
- To investigate the influence of vegetation distribution on the velocity shear and turbulence generation.

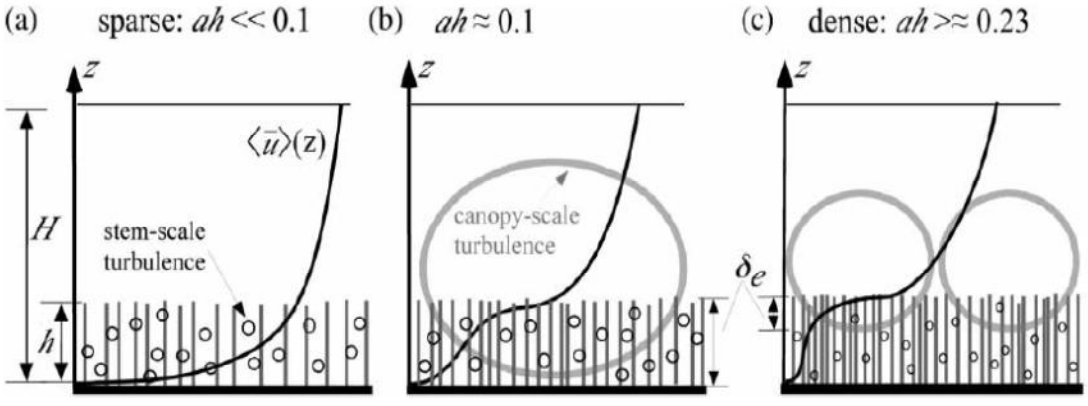


**Fig. 1. The mean velocity profiles in submerged vegetation with increasing stem density [7]**

## 2. EXPERIMENTAL METHODS

The experiments were conducted in 22mm long rectangular re-circulating flume of width $B = 614mm$ at the University of Birmingham. The channel is supplied from a constant head tank with a capacity of $45{,}500l$ in the laboratory roof. Two flow discharges ( $Q$) were investigated ($30.0\ l/s$ and $30.50\ l/s$) with corresponding flow depths ($H$) of $130mm$ and $128mm$ and width to depth ratios ($^{B}/_{H}$) of $4.7$ and $4.8$ respectively to achieve subcritical flow condition. In what follows these experimental conditions are referred to as EXPT1 and EXPT2 respectively. The corresponding water surface slopes for EXPT1 and EXPT2 were 0.0008 and 0.0011 $\pm 0.0001$ respectively. Detailed velocity measurements were made at three cross sections (CRS1, CRS2 and CRS3) at distances of 17.5m, 17.85m and 18.2m respectively downstream from the channel inlet. In the results that follow, the gravel region of the bed extends over $(0 \leq {}^{y}/_{B} \leq 0.5)$, the interface occurs at $({}^{y}/_{B} = 0.5)$, and the vegetated region extends over $(0.5 \leq {}^{y}/_{B} \leq 1.0)$, where $y$ is the lateral distance from the left hand side looking downstream and $B$ is the channel width. The streamwise direction $x$ is in the direction of flow. The transverse direction $y$ is perpendicular to x in the lateral direction, while the vertical direction is denoted by $z$ and is perpendicular to the $xy$ plane (positive upwards). The corresponding time average velocity components are $U,V,W$ respectively with the associated fluctuating velocity components defined as $u',v',w'$ respectively.

### 2.1 Vegetation Types and Roughness Generation

Two different types of idealised vegetation are examined in conjunction with the gravel roughness ($D_{70}$=*10mm*), i.e., idealised grass formed using artificial grass (Astroturf) and rigid vegetation arranged in a staggered grid formed from plastic (see Table 1 and Fig. 2). In keeping with the work of [4] the vegetation and gravel form patches of width 0.307m and length 1.825m and alternate in a checkerboard formation down the channel (Fig. 2).

### 2.2 Data Collection

#### 2.2.1 Velocity measurement

Velocity measurements were undertaken at all three cross sections (CRS1, CRS2, and CRS3), using a Nortek acoustic Doppler velocimeter (ADV) and $4mm$ diameter Pitot static tube for the free surface and within the vegetation. The ADV measures simultaneously the three velocity components at a frequency of 200Hz. A convergence test was performed to obtain an optimum sampling period at each measurement point (i.e., 60 seconds). For each cross section a vertical profile of velocity data was collected from the middle of the channel towards the channel sidewalls at $10mm$ horizontal and vertical spacing resulting in approximately 495 measured points for a cross section. For each vertical profile the maximum measurable height with ADV was $5cm$ below the free surface.

## 3. RESULTS

### 3.1 Mean Velocity Profiles and Distribution

The mean velocity ($U_m$) was obtained for each measured point and normalized by the bulk mean velocity $(U_{Q/A})$ where *A* is the cross sectional area. To provide an indication of the degree of reliability of the data collected, the time averaged velocity data at each point was numerically integrated and compared to $U_{Q/A}$. For EXPT1 and EXPT2 the difference was 3% and 2.8% respectively; this was considered appropriate for the current work and is comparable with [4].

Fig. 3 shows transverse profiles of streamwise velocity for selected elevations. With regards to EXPT1 the grass vegetation retards the transverse profiles relative to gravel bed, while the minimum averaged velocity appears at the roughness interface region in EXPT2. Generally it can be seen that all transverse profiles indicate a change in lateral shear (i.e. changes in dU/dy at the interface $({}^{y}/_{B} = 0.5)$ between the gravel and vegetated sections. As indicated in Fig. 3,

**Table 1. Summary of vegetation roughness properties**

| | Height | Width | Thickness | Density |
|---|---|---|---|---|
| EXPT1-Grass | $26mm$ | $1mm$ | $0.15mm$ | $15625 plants/m^2$ |
| EXPT2-Rigid | $26mm$ | $15mm$ | $10mm$ | $800 plants/m^2$ |


**Fig. 2. Two model vegetation simulated with gravel roughness: EXPT1( left upper); EXPT2 (right upper) and the plan view showing the three cross sections measured**

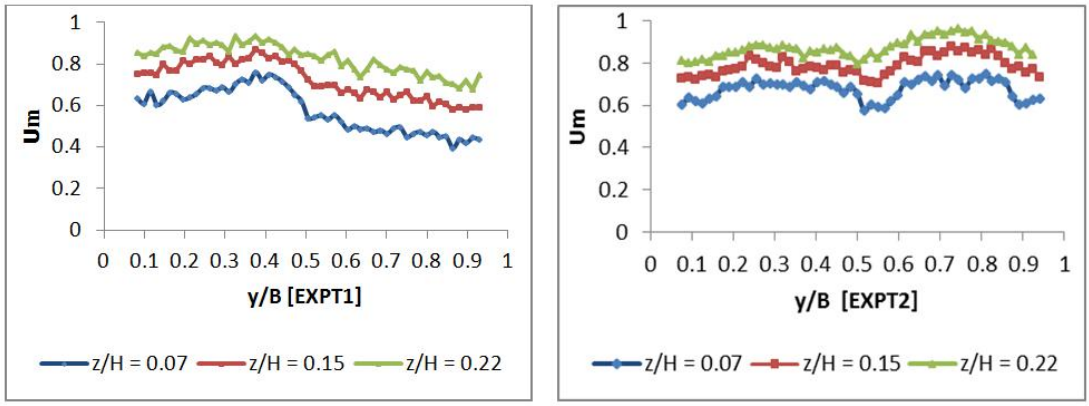


**Fig. 3. Lateral velocity profiles CRS3: (a) EXPT1, (b) EXPT2**

increased lateral shear is more pronounced in EXPT1 (artificial grass) compared to the EXPT2 (rigid boundary). What is also interesting is the indication in EXPT2 that the gravel surface is rougher than the rigid vegetation.

Fig. 4 compares the vertical mean velocity $(U_m)$ profiles for three cross sections over the vegetated and gravel bed. It can be seen from the figure that the presence of vegetation retards the flow near bed with much lower value over the vegetated region $\left({}^{y}/_{B} = 0.65\right)$ relative to gravel region $\left({}^{y}/_{B} = 0.19\right)$ in EXPT1. This is attributed to the slow velocity flow within the vegetation due to stem density and the resulting vertical shear as further examined in the subsequent results. In EXPT2, the mean velocities are approximately constant over a large proportion of the two bed roughness at a given height as illustrated in Fig. 4. The effect of the near bed accelerated flow on the vertical shear in EXPT2 is given in the discussion section.

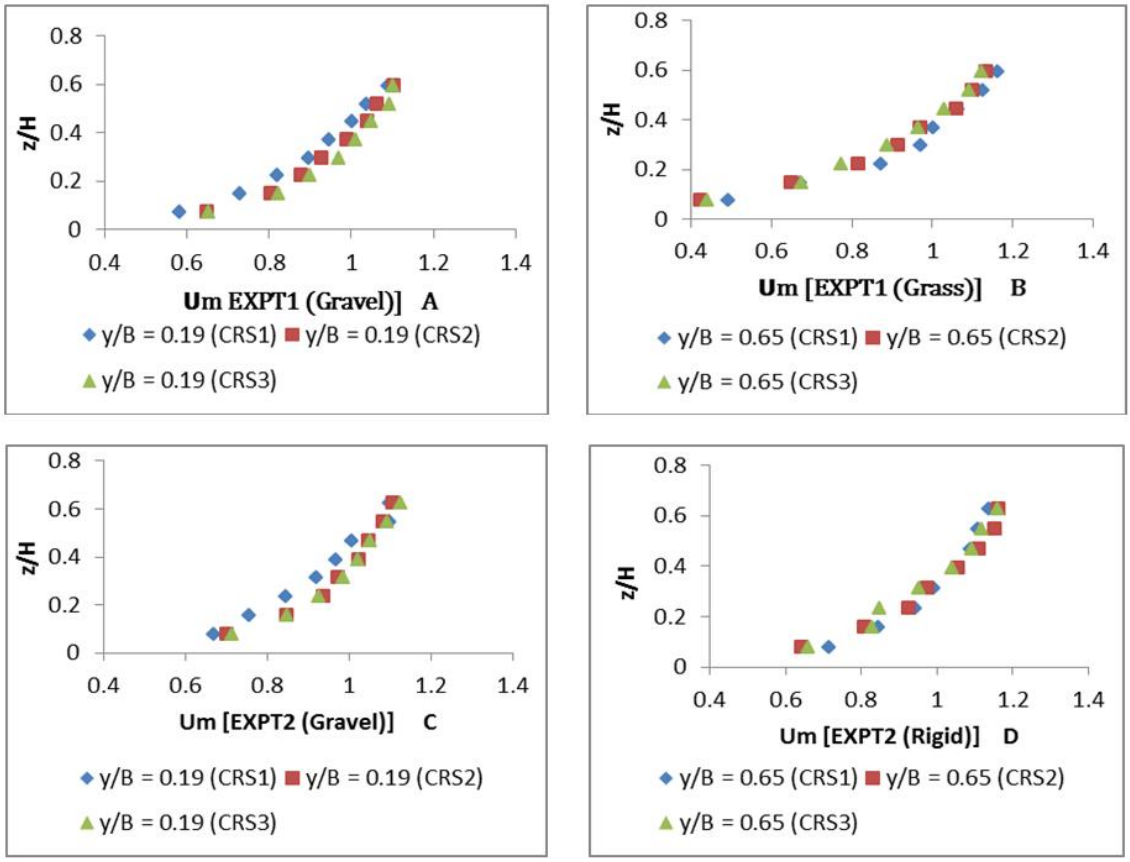


**Fig. 4. Selected vertical profiles of mean velocity from CRS1, CRS2 and CRS3: EXPT1 and EXPT2**

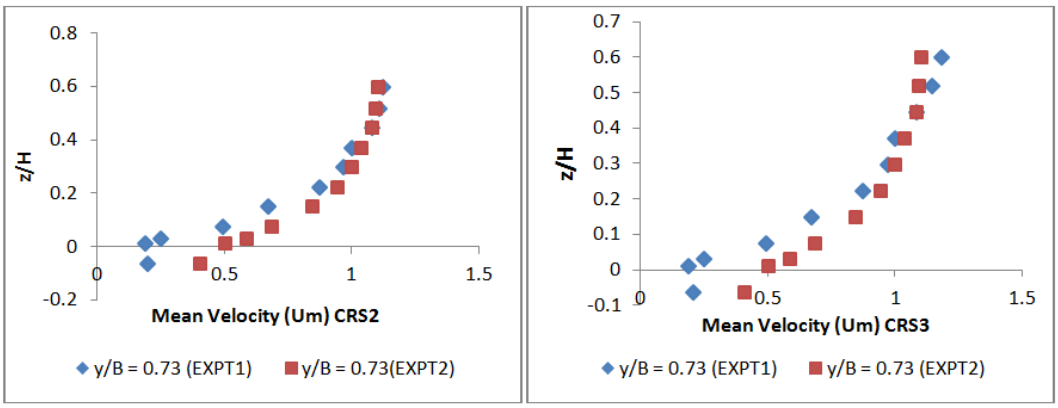


**Fig. 5. Vertical velocity profiles over vegetated bed with porous layer for cross section one and two**

The vertical profiles of the mean velocity over vegetated bed is explored further to examine the flow existence within the vegetated bed, measurements were undertaken for three vertical points using a Pitot - static tube $4mm$ diameter. The vertical velocity profiles are shown in Fig. 5. Vegetation stems were removed within an area $0.03m^2$ to allow the tube into vegetation zone.

The flow within the vegetation is at a smaller spatial scale $\left({}^{z}/_{H} \leq 0.07\right)$ but the measurements revealed low velocities compared to the value at the vegetation top as measured using the ADV forming two layer flows over vegetated bed given an indication of vertical shear. The analysis of the dynamics of vertical with horizontal shear is given in the discussion section.

Fig. 6 shows the secondary flow distributions for EXPT1and EXPT2. The maximum measured secondary flow vector is within $3\%$ of the mean streamwise velocity for both experiments and is in keeping with the findings of [4,6,9]. Visual inspection shows that the magnitude of secondary flow over the gravel bed in EXPT1 is large with occurrence of down-flow, and up-flow over the grass bed. At the lower region $\left({}^{z}/_{H} \leq 0.2\right)$of the flow, the transverse motion is directed from the gravel bed towards the grass bed, and at the upper region $\left({}^{z}/_{H} > 0.2\right)$ , the flow is transported laterally in opposite direction. The secondary flow vectors in EXPT2 suggests the presence of circulating cells moving in clockwise direction [4,6,7,10,9] with a strong up-flow at the roughness interface$\left({}^{y}/_{B} = 0.5\right)$, the flow cells in clockwise direction appear to dominate momentum transfer between the bed strips Fig. 6. The up-flow corresponding to the low velocity flow over vegetated region in Fig. 4 may be caused by the retardation of the flow near bed by the grass vegetation.

### 3.2 Profiles of Reynolds Stress

Fig. 7 compares the vertical profiles of vertical Reynolds stress $\left(-\overline{u'w'}/\tau_b\right)$ where $u'$ and $w'$ are streamwise and vertical fluctuating velocities respectively. The mean boundary shear stress $\tau_b$ was evaluated as $\rho g R S_0$ where $\rho$ is the water density, $g$ is the acceleration due to gravity, $R$ is the hydraulic radius and $S_0$ is the bed slope. Over the gravel bed $\left(0 \leq {}^{y}/_{B} \leq 0.5,\right)$ the vertical Reynolds stress has a local maximum above the bed at approximately $\left({}^{z}/_{H} \cong 0.2\right)$, after which it decays in approximately linear fashion towards the channel bed and the free surface from the maximum point. This is in good agreement with the wall region as defined [10]. In this region the vertical Reynolds stress decreases towards the channel bed due to the presence of non-negligible viscous shear stress induced by the bed surface [7]. Moreover, the near bed momentum transport from gravel bed to the vegetated bed is assumed to have contributed to the reduced value of the near bed shear stress over the gravel bed. This is observed to have contributed to the momentum balance in the near bed flow region [11].

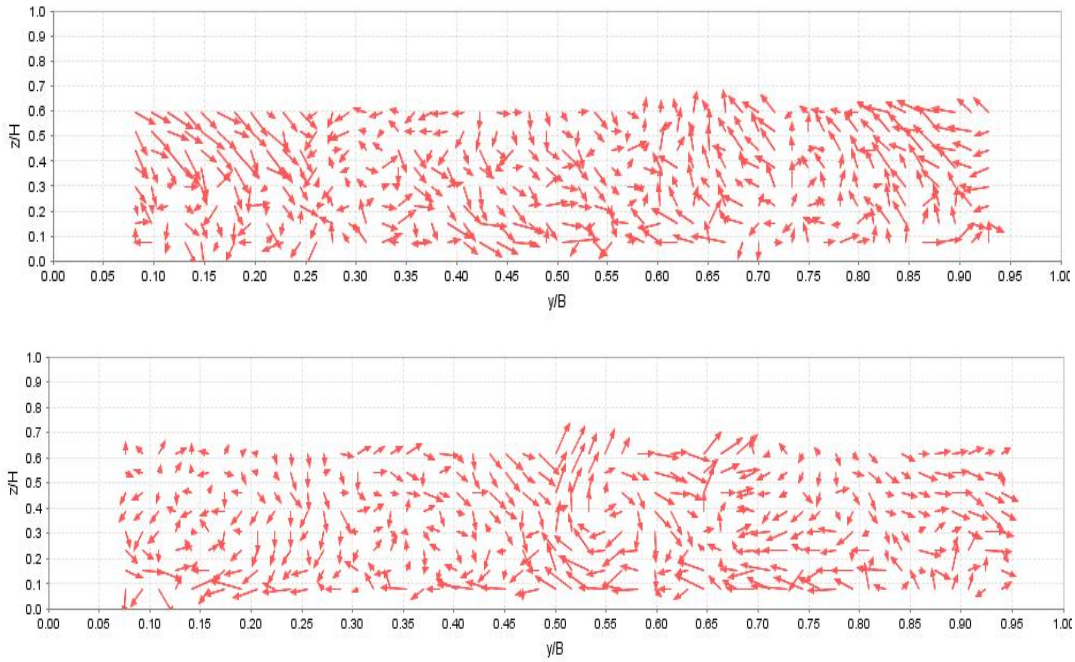


**Fig. 6. Secondary flow distribution CRS3: EXPT1 (upper), EXPT2 (lower)**

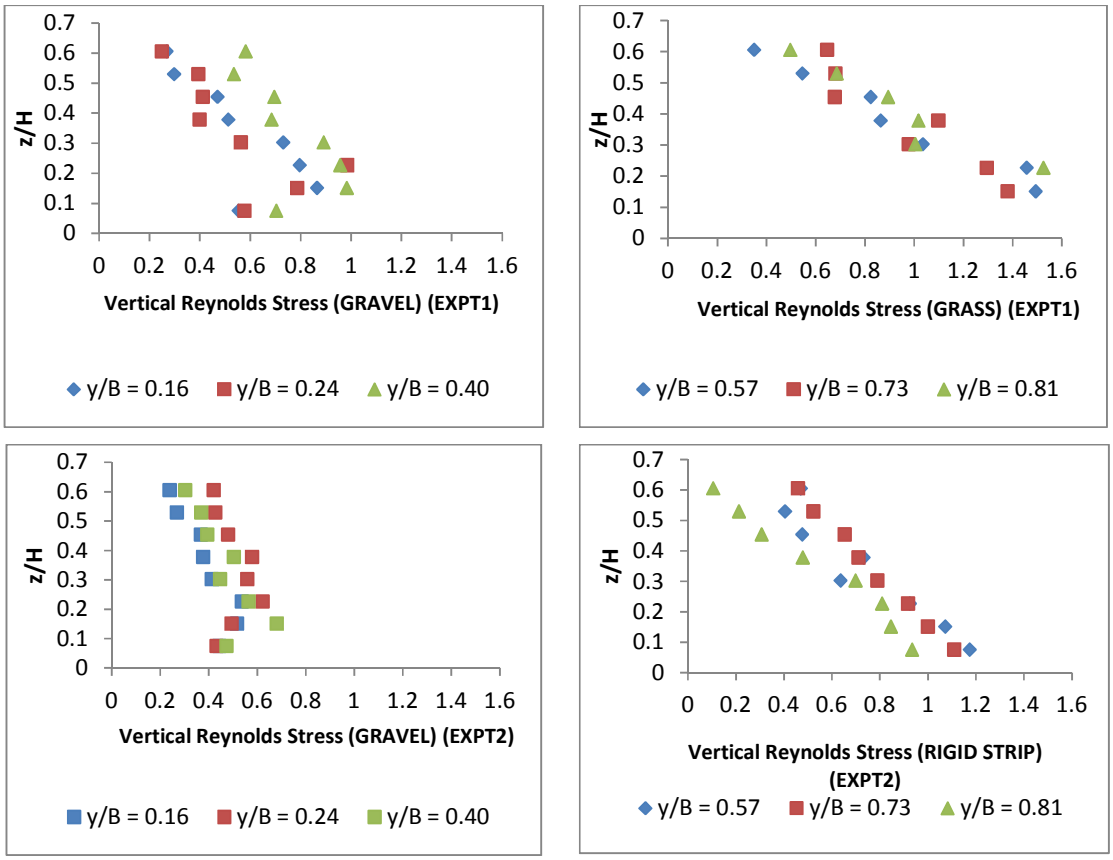


**Fig. 7. Vertical profiles of Vertical Reynolds stress by bed: EXPT1 (top), EXPT2 (down)**

Over the vegetated bed $(0.5 \leq {}^{y}/_{B} \leq 1.0)$, the vertical Reynolds stress is reasonably linear over the measured section, with a maximum value occurring close to the channel bed. This behaviour is consistent with an inflection point in a submerged vegetation which is characterized by a shear layer and possibly indicates the existence of a 'wake layer' below the vegetation surface roughness as shown in Fig. 5; thus, the effective height of the bed lies below the roughness crest [12],

Fig. 8 shows contours of the horizontal Reynolds stress $(-\overline{u'v'}/\tau_b)$ where $v'$is the lateral fluctuating velocity. The figure indicates the existence of the horizontal Reynolds stress over the vegetated bed. The shear propagation across the bed and towards the gravel zone is apparent; this may be attributed to the vertical orientation of vegetation stems enhancing small scale horizontal turbulence due to stem wakes within vegetation. Comparing Fig. 6 and Fig. 8, it can be seen that the region of maximum (negative) horizontal Reynolds stress correspond with the up-flow regions.

In addition, the horizontal Reynolds stress is maximized at the roughness interface region $({}^{y}/_{B} = 0.5)$ of the flow in EXPT2.

## 4. DISCUSSION

### 4.1 Vegetated and Roughness Interface Shear Layer Flow

The dominant factor influencing turbulent transport in open channel flow is the degree of velocity shear due to different roughness sections. In this paper, Reynolds stresses are assumed as indicators of turbulence transport effects [13].

The presence of both vertical and horizontal shear is notable in this work from Figs. 3 and 5; efficient vertical transport of momentum across the shear layer through the vegetation-water interface region $({}^{z}/_{H} \leq 0)$relative to gravel bed is expected due to the vertical shear over the vegetated bed as shown in Fig. 5. Similarly, there is evidence of horizontal shear at the roughness

interface regions $(^{y}/_{B} = 0.5)$ as shown by the lateral velocity profiles. In such condition turbulence transfer is expected over the roughness interface region.

Referring to Fig. 7, the vertical profiles of Reynolds stress exhibit a strong peak at the position of the vegetation top; this height coincides with the inflection point in the velocity profile in Fig. 5. The shear layer is featured in this work by the point of the maximum Reynolds stress at the top of vegetation as shown in the vertical distributions of the vertical Reynolds stress in Fig. 7. It should be noted from the figures that the vertical Reynolds stress exhibits more peak over the vegetated bed in EXPT1 than in EXPT2.

Fig. 9 compares the depth averaged vertical and horizontal shear stresses. The figure illustrates greater magnitude of vertical shear over the vegetated grass bed relative to the gravel bed in EXPT1; this is assumed to enhance turbulence in the vertical plane due to increased vegetation density. Also noted is the negative lateral momentum transport at the interface region $(^{y}/_{B} = 0.5)$, the vertical shear over vegetated bed in EXPT1 is assumed to have suppressed the level of horizontal shear at the interface region in contrast to [6] where the momentum transfer is maximized at the rough-smooth boundary.

In EXPT2, the horizontal turbulent shear stresses attain a maximum at the roughness interface region $(^{y}/_{B} = 0.5)$ which is consistent with the results in Figs. 6 and 8.

### 4.2 Bursting Mechanism by Quadrant Analysis

To investigate the coherent structure due the multiple shear layer induced by vegetation, a quadrant conditional analysis as proposed by [12] for instantaneous Reynolds stress is applied. The quadrant Reynolds stress $\boldsymbol{QR_i}$ is defined as follows:

$$QR_i = lim\frac{1}{T}\int_o^T \big(u'(t).v'(t)\big)I(t)dt \qquad (i = 1,2,3,4) \tag{1}$$

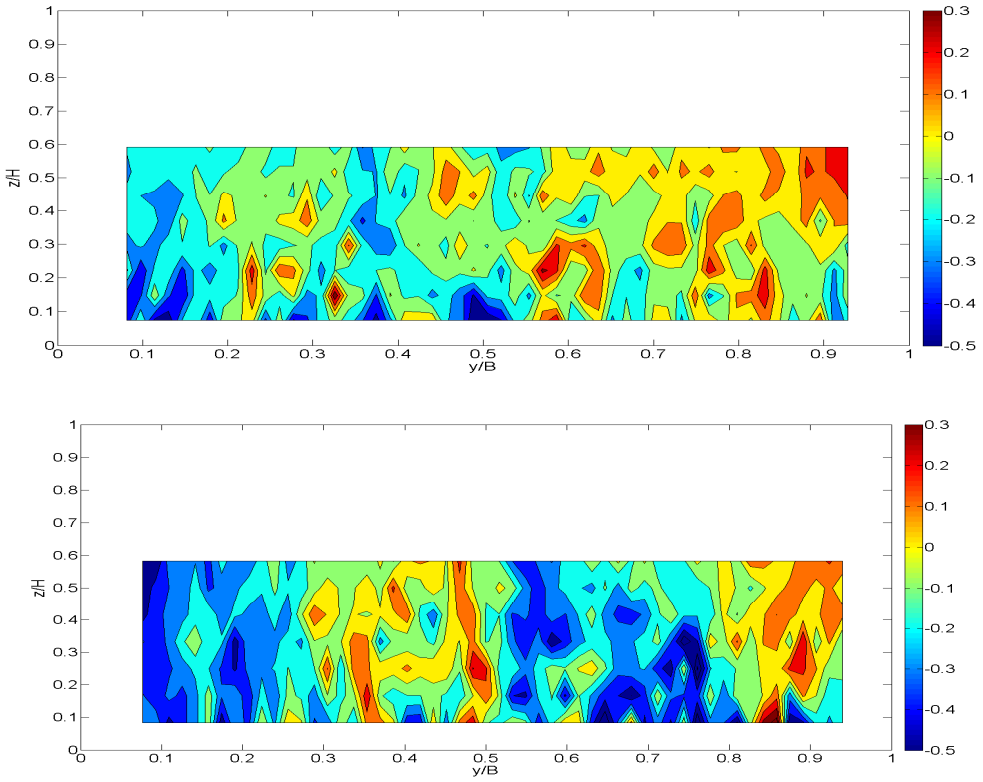


**Fig. 8. Distribution of Relative Horizontal Reynolds stress: EXPT1 (upper), EXPT2 (lower)**

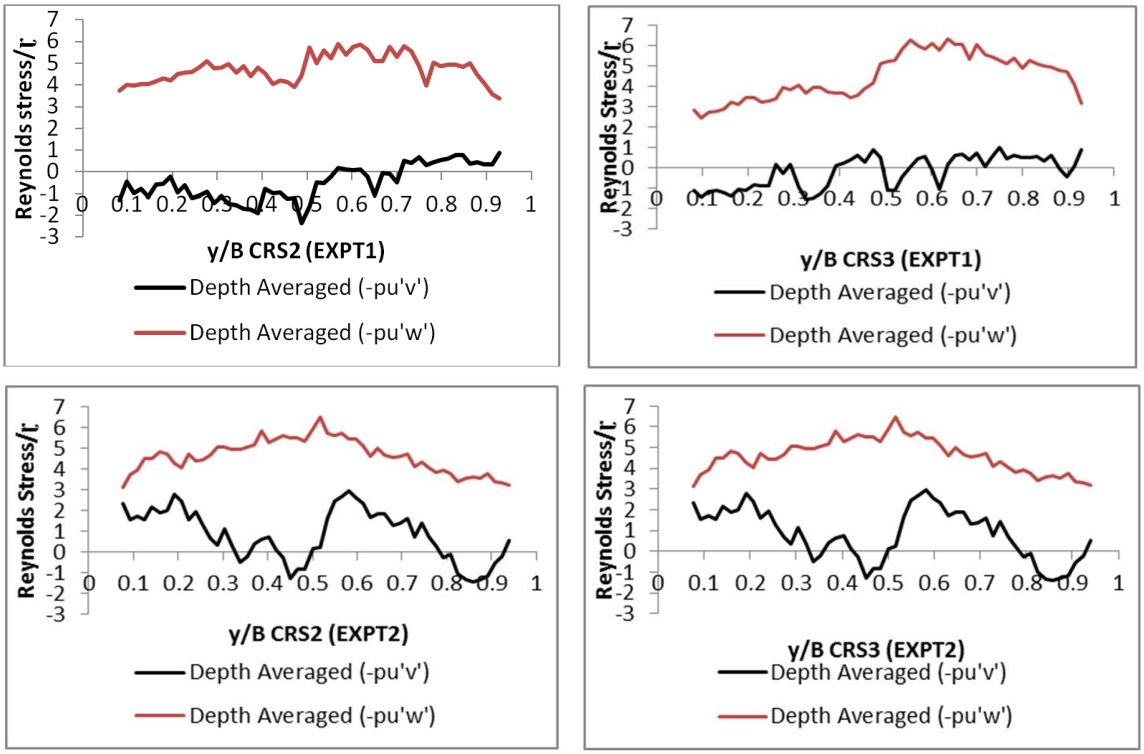


**Fig. 9. Lateral Distribution of depth averaged horizontal and vertical shear stresses for EXPT1 and EXPT2**

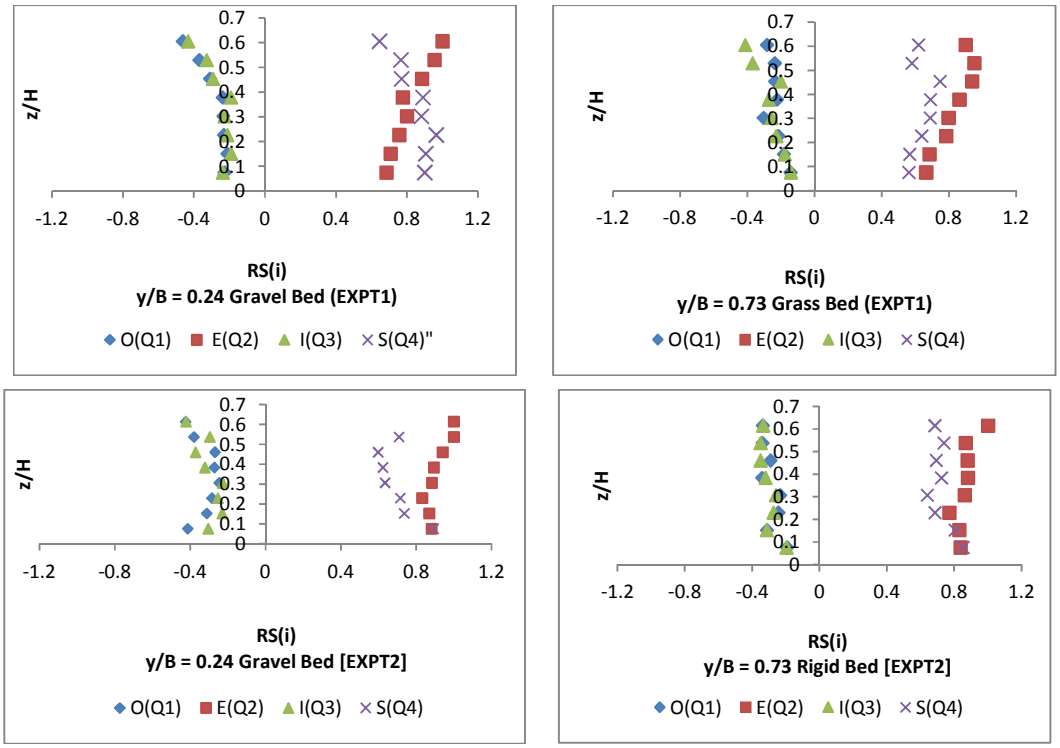


**Fig. 10. Quadrant Reynolds Stress distribution over gravel and vegetated beds: EXPT1 (top), EXPT2 (down)**

The quadrant analysis divides the paired time series data into four quadrants based on the signs of the fluctuating velocity components. In this research the following analyses describes the pair of streamwise velocity fluctuation $(u')$ and vertical velocity fluctuation $(w')$ components in each quadrant. The existence of pair fluctuating components $(\boldsymbol{u}', \boldsymbol{w}')$ defines event in quadrant $i$, $I$ provides indication of right event in a quadrant $\boldsymbol{i}$. If fluctuating components $(\boldsymbol{u}', \boldsymbol{w}')$ exists in a quadrant $i$, then $\boldsymbol{I_i = 1}$, otherwise $\boldsymbol{I_i = 0}$. Each quadrant is defined for the following events:

$i = 1(u' > 0, w' > 0)$: Outward interaction of high velocity
$i = 2, (u' < 0, w' > 0)$: Ejections of low velocity flow
$i = 3, (u' < 0, w' < 0)$: Inward interactions of low velocity flow
$i = 4(u' > 0, w' > 0)$**:** Sweep

Fig. 10 show the vertical distributions of the quadrant Reynolds stress $Q_i$ normalized by the bulk shear stress for selected sections over gravel bed $(y/_B = 0.24)$ and vegetated bed $(y/_B = 0.73)$ for EXPT1 and EXPT2 respectively. The Reynolds stress contribution analysis demonstrates that ejection $(Q_2)$ and sweep $(Q_4)$ events are the most evident dominant contributors to the Reynolds shear stress. This observation is consistent with the previous research works(Nezu and Nakagawa, 1993). However the contributions of$(Q_1)$ and $(Q_2)$ events are predominantly negative. In EXPT1 Fig. 10 (top), the distributions of sweep $(Q_4)$ and ejection $(Q_2)$ have their maximum values over the gravel and the vegetated bed, Ejection motions $(Q_2)$ dominates Sweep motions over grass vegetated bed by exhibiting much larger value than Sweep $(Q_4)$ over the grass vegetated bed, it should be noted that the Ejection motions transport the low velocity flow over the grass bed up to the free surface, this supports the upward secondary flow as observed in Fig. 6, and over the gravel bed the Sweep motions dominates Ejection motions. At the upper region of the flow, Ejection motions generally dominate the flow and turbulence transport. Similar distributions are observed in EXPT2 where Ejections and Sweeps dominate the flow Fig. 10 (down). The Sweep motions are more significant near bed while Ejections dominates the flow at the upper region of the flow. In both experiments, the contributions of the inward $(Q_1)$ and outward $(Q_3)$ interactions are negligibly small and negative. This result implies that Ejection and Sweep events are most evident in similar manner as observed in boundary layer problems in open channel flows. Relative to EXPT1, the peak values of Ejection $(Q_2)$ in EXPT2 becomes smaller; this supports the observation of smaller vertical momentum exchange in EXPT2 in comparison to EXPT1. It has been observed in the literature [7] that vertical shear layer generation is directly proportional to the density and distribution of vegetation elements.

## 5. CONCLUSIONS

This research extends the work of [4,6] by considering the effect of idealized vegetation on the flow characteristics of a heterogeneous open channel. The study present results of experiments with two different types of idealised vegetation patches with gravel roughness. In EXPT1 idealised grass is formed using artificial grass (Astroturf) and rigid vegetation arranged in a staggered grid formed from plastic material in EXPT2.

The research has highlighted the following based on the objectives;

- The vertical profiles of the mean velocity show lower mean velocities near bed over vegetated bed in EXPT1 as shown in Fig. 4, furthermore it is shown in Fig. 5 that the grass stem density increases the retardation of the flow within the vegetation. Therefore, the magnitude of the velocity difference within and over the vegetation become more effective in promoting vertical turbulence
- In keeping with the previous work [6], the lateral interaction and transport is achieved by the secondary flow, at the lower region $(z/_H \leq 0.2)$ of the flow, the transverse motion is directed from the gravel bed towards the grass bed, and at the upper region $(z/_H > 0.2)$, the flow is transported laterally in the opposite direction in EXPT1. The secondary vector in EXPT2 suggests the presence of circulating cells moving in clockwise direction as illustrated in Fig. 6.
- In EXPT1, the presence of vegetation promotes vertical shear and the resulting dominance of vertical momentum transport as illustrated in Fig. 7. Applying a force balance to the depth averaged the momentum equation; the dominance of vertical momentum transport over the vegetated bed is shown to suppress the

lateral momentum transport at the roughness interface $(^{y}/_{B} = 0.5)$ as shown in Fig. 9.

- In EXPT2, the distribution of the vegetation elements to achieve a staggered pattern created less a dense flow domain within the vegetation which reduced the vertical shear over the vegetated bed relative to EXPT1 (Fig. 5). This is assumed to enhance the lateral momentum transfer at the roughness interface region similar to [4] as illustrated in Figs. 8 and 9. This indicates that the roughness distribution has an enhanced impact on turbulence generation compared to the magnitude of the surface roughness.
- As shown in Fig. 7, the velocity shear and turbulence resulting from the boundary effect over the gravel bed are dominated by the vegetation generated turbulence.
- The study demonstrates that relative to turbulence distribution, the vegetated bed exerts a major influence on the flow.
- From the results, local regions of efficient moment transport can be predicted in natural rivers with similar patches of roughness.

## ACKNOWLEDGEMENTS

Financial support was provided by the Tertiary Education Fund (TETFUND) Nigeria. Authors graciously acknowledge and appreciate the support.

## COMPETING INTERESTS

Author has declared that no competing interests exist.

## REFERENCES

1. Lopez F, Garcia M. open-channel flow through simulated vegetation: suspended sediment transport modelling. Water Resour. Res. 1998;34:2341-2352.
2. Water Resources Research. 46:(w04504): 1-14.
3. Ghisalberti M, Nepf HM. The structure of shear layer flow flows over rigid and flexible canopies. Environ Fluid Mech. 2006;6(3): 277-301.
4. Jesson M, Sterling M, Brigdeman J. Modelling Flow in an Open Channel with Heterogeneous Bed Roughness. Journal of Hydraulic Engineering. 2013;139:195-204.
5. Knight DW, Omran M, Tang X. Modeling Depth-Averaged Velocity and Boundary Shear in Trapezoidal Channels with Secondary Flows. Journal of Hydraulic Engineering. 2007;133:39-47.
6. Jesson M, Sterling M, Bridgeman J. An experimental Study of Turbulence in a Heterogeneous Channel. Water Management Proceedings of the Institution of Civil Engineers. 2012;166:(WM1):16-26.
7. Nepf HM. Hydrodynamics of vegetated channels. Journal of Hydraulic Research. 2012;50:(3):262-279.
8. Ghisalberti M, Nepf HM. Mixing layers and coherent structures in vegetated aquatic flows. Journal of Geophysical Research. 2002;107:(C2).
9. Wang ZQ, Cheng NS. Secondary flows over artificial bed strips. Advances in Water Resources. 2005;28:441-450.
10. Nezu I, Nakagawa H. Cellular Secondary Currents in Straight Conduit. Journal of Hydraulic Engineering. 1984;110:173-193.
11. Shiono K, Knight DW. Turbulent open-channel flows with variable depth across the channel. J. Fluid Mech. 1991;222:617-646.
12. Nezu I, Nakagawa H. Turbulence in Open Channel Flows. Rotterdam, A.A. Balkema, (Rotterdam, A.A. Balkema); 1993.
13. Shucksmith JD, Boxall JB, Guymer I. Effects of emergent and submerged natural vegetation on longitudinal mixing in open channels; 2010.

*© 2018 Folorunso; This is an Open Access article distributed under the terms of the Creative Commons Attribution License (http://creativecommons.org/licenses/by/4.0), which permits unrestricted use, distribution, and reproduction in any medium, provided the original work is properly cited.*

*Peer-review history:*
*The peer review history for this paper can be accessed here:*
*http://www.sciencedomain.org/review-history/23270*